Computer-originated aspheric holographic optical elements

R. C. Fairchild*
J. R. Fienup
Environmental Research Institute of Michigan
Radar and Optics Division
P.O. Box 8618
Ann Arbor, Michigan 48107

Abstract. Holographic optical elements (HOEs) recorded with arbitrary aspheric wavefronts can now be analyzed with a holographic ray-tracing design program. The recording wavefronts are defined by analytical phase functions, for example, a two-dimensional polynomial expansion. The coefficients of the functional representations of the HOE recording wavefronts are used as parameters to optimize the performance of an optical system containing the HOE. The optimum recording wavefronts are then produced with the help of computer-generated holograms. Several useful arbitrary wavefront phase functions are discussed. Design predictions and experimental results are presented for a holographic Fourier transform lens recorded with the aid of a computer-generated hologram.

Keywords: holographic optical elements; computer-generated holograms; diffractive optics; lens design.

Optical Engineering 21(1), 133-140 (January/February 1982)

CONTENTS

1. INTRODUCTION

The increased use in many applications of refractive optical elements having aspheric surfaces has produced optical systems with better performance and fewer elements when compared with systems containing only spherical surfaces. It is reasonable to suppose, therefore, that holographic optical systems would also benefit from the use of aspheric holographic optical elements (aspheric HOEs). In this case the word "aspheric" refers to the wavefronts used to record the HOE rather than the substrate upon which the HOE is recorded.

*Currently with Kaiser Optical Systems, Inc., A Kaiser Aerospace and Electronics Company, P.O. Box 983, Ann Arbor, Michigan 48106.

Paper 1790 received Apr. 28, 1981; revised manuscript received June 17, 1981; accepted for publication June 26, 1981; received by Managing Editor July 6, 1981. This paper is a revision of Paper 215-01 which was presented at the SPIE seminar on Recent Advances in Holography, Feb. 4-5, 1980, Los Angeles, CA. The paper presented there appears (unrefereed) in SPIE Proceedings Vol. 215.

The design of diffractive optical systems has until recently been restricted to the use of HOEs recorded with spherical wavefronts (including the plane wavefront, which is considered a spherical wavefront with infinite radius of curvature), as depicted in Fig. 1. Aspheric HOEs may now be designed with recording wavefronts derived from auxiliary optical systems (Fig. 2(a)) or with truly arbitrary wavefronts defined analytically (Fig. 2(b)). In the latter case it may be difficult at best to generate a truly arbitrary recording wavefront using standard refractive optical components. A more feasible approach to generating an arbitrary aspheric wavefront is through the use of a computer-generated hologram (CGH).[1] The increasing availability and performance of devices for recording CGHs make this an attractive approach.

This paper describes the implementation of an aspheric HOE design capability within an existing holographic ray-trace program. Consideration is given to methods for defining arbitrary recording wavefronts on curved as well as flat substrates. In addition, techniques for defining CGHs to generate the desired arbitrary recording wavefronts are presented. Finally, the design of a simple aspheric HOE to be used as a Fourier transform lens is described and experimentally evaluated.

2. RAY TRACING THROUGH HOEs

It is important to recognize that three different optical systems are involved in the analysis of a HOE. The optical system in which the HOE is employed is referred to as the "primary system." Additional optical systems are required to form each of the two wavefronts, the object beam and the reference beam, used to record the HOE. Often a recording wavefront is a spherical wavefront, in which case the "optical system" is nothing more than free-space propagation from a point source of light to the HOE. More generally, a recording

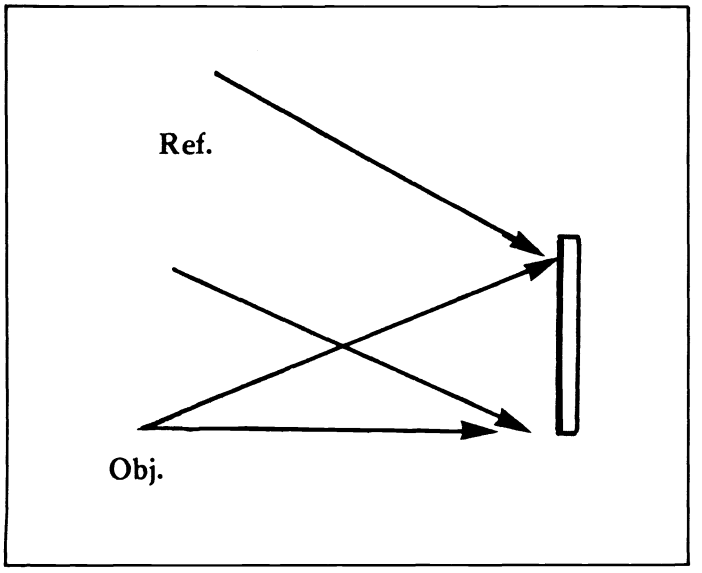

Fig. 1. Conventional (spherical) HOEs are recorded with spherical and/or plane wavefronts.

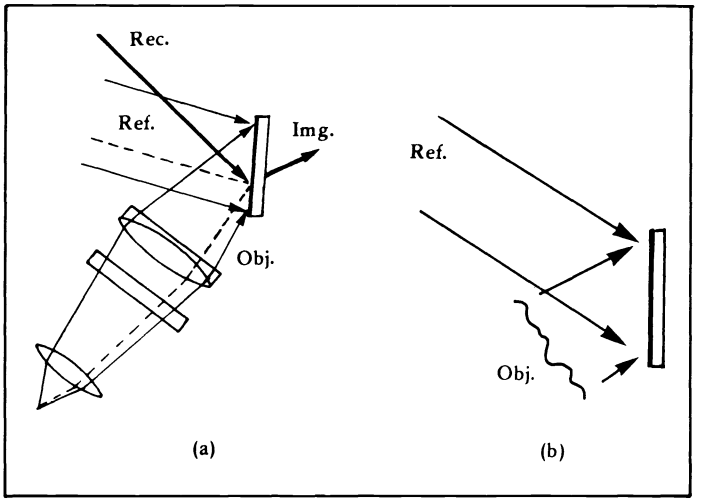

Fig. 2. Aspheric HOEs are recorded with an object wavefront (a) derived from an auxiliary optical system or (b) defined analytically.

wavefront can be defined by an auxiliary optical system, as depicted in Fig. 2(a), for example.

A short discussion of the ray-trace grating equations is appropriate at this point. In Fig. 2(a) the object wavefront (Obj.) is shown to be derived from an auxiliary optical system, and the reference wavefront (Ref.) is a plane wave. During the ray trace through the primary optical system, a reconstruction ray (Rec.) impinges upon the hologram, is diffracted by the hologram, and results in an image ray (Img.). The phase and direction of propagation of the image ray is determined by the phases and directions of the reconstruction, reference, and object rays at the reconstruction ray intercept. The hologram is assumed to lie in the x-y plane. A simplified form of the grating equations which determine the image ray is as follows:

$$\phi_I = \phi_C \pm (\phi_O - \phi_R) \; ; \tag{1}$$

$$l_I = l_C \pm \frac{\lambda_C}{\lambda_O}(l_O - l_R) \; ; \tag{2}$$

$$m_I = m_C \pm \frac{\lambda_C}{\lambda_O}(m_O - m_R) \; ; \tag{3}$$

and

$$n_I = \pm \sqrt{1 - l_I^2 - m_I^2} \; , \tag{4}$$

where ϕ is the ray phase; λ_C is the readout wavelength; λ_O is the recording wavelength; l, m, and n are the x, y, and z direction cosines, respectively; and subscripts I, C, O, and R refer to the image, reconstruction, object, and reference rays, respectively. All wavelengths considered in this paper are the wavelengths within the recording medium. The sign choice in Eqs. (1)–(3) is used to select either the principal diffracted wavefront (+) or the conjugate wavefront (−). The sign choice in Eq. (4) is used to select the z-direction of propagation of the wavefront.

In a typical ray-trace problem, the phase and direction cosines of the reconstruction ray are known, either as inputs to the system or as the result of ray tracing through a preceding element. The phases and direction cosines of the object and reference rays, however, must be determined based upon the reconstruction ray intercept. For the case of a spherical HOE, in which the object and reference wavefronts are restricted to being either plane or spherical wavefronts, the task is a simple one. The phase and direction cosines of a ray passing through any point in space are easily calculated based upon the direction of the plane wavefront or the location of the spherical point source. The case of an aspheric HOE, however, may present a more difficult task depending upon the way in which the arbitrary recording wavefront is defined.

The two principal ways of defining an arbitrary wavefront are (1) by the specification of an auxiliary optical system that is used to generate the wavefront (Fig. 2(a)), or (2) by an analytical description of a wavefront defined on a surface (Fig. 2(b)). In this paper we discuss both ways of describing arbitrary recording wavefronts, with emphasis on the analytical description.

3. ARBITRARY RECORDING WAVEFRONTS DERIVED FROM AUXILIARY OPTICAL SYSTEMS

The task of determining the phase and direction cosines of a recording wavefront derived from an auxiliary optical system at a given reconstruction ray intercept is indeed a difficult one. There are two basic approaches to solving this problem. The first approach is to trace rays through the auxiliary system in an iterative fashion until the ray which passes through the reconstruction ray intercept is found. The second approach is to trace a grid of rays through the auxiliary system to the HOE, and then, during the ray tracing of the primary system, to perform an interpolation on the grid of rays to obtain the phases and direction cosines at the reconstruction ray intercepts.

Each of the above approaches has its own advantages and disadvantages. The iterative approach requires that several rays be traced through the auxiliary system for each ray that is traced through the primary system. In general, the number of iterative ray traces through the auxiliary system for each primary system ray trace will be small since the arbitrary recording wavefronts of interest for HOEs are usually well behaved. The interpolation approach, on the other hand, requires that a relatively large number of rays (typically 25 to several hundred) be traced through the auxiliary system once. Thereafter, any number of rays may be traced through the primary system, and only interpolation will be required to determine the phase and direction cosines of the arbitrary recording wavefront at each reconstruction ray intercept. A two-dimensional interpolation is required which preferably takes into account the known direction cosine samples as well as the phase samples. The interpolation is further complicated by the fact that a regularly spaced grid at the input to the auxiliary optical system will be distorted into an irregular grid at the HOE. If the auxiliary system contains an optimization variable, the grid of rays will need to be retraced each time the

variable changes value. The tradeoffs between the two approaches are complex and depend in large part on the relative complexities of the primary and auxiliary systems.

Both approaches have been implemented within the Holographic Optics Analysis and Design (HOAD)[2] program at ERIM. The interpolation approach is discussed in detail in Ref. 3. The remainder of this paper will concentrate on the class of aspheric HOEs for which the arbitrary recording wavefronts are defined analytically at the recording surface.

4. ANALYTICAL ARBITRARY WAVEFRONTS FOR ASPHERIC HOE DESIGN

We have recently added to the HOAD ray-trace program at ERIM the capability of analyzing aspheric HOEs recorded with analytically defined wavefronts. The analysis is currently limited to recording wavefronts which are pure phase functions, i.e., the wavefront amplitude is assumed uniform over the extent of the wavefront. The phase function is assumed to be defined on the surface of the recording medium. The surface (or substrate) can be flat or curved. A variety of general analytical phase functions have been supplied for the designer's use including the following:

- Sum of monomials (power series)

$$\phi(x,y) = \sum_{i=0}^{9} \sum_{j=0}^{9} C_{ij}\, x^i y^j \tag{5}$$

- Sum of Legendre Polynomials (orthogonal polynomials)

$$\phi(x,y) = \sum_{i=0}^{9} \sum_{j=0}^{9} C_{ij}\, L_i(x) L_j(y) \tag{6}$$

- Spherical wavefront + sum of monomials
- Spherical wavefront + sum of polynomials .

The C_{ij} in Eqs. (5) and (6) represents the coefficient values of the respective polynomials. Up to 100 coefficients may be specified for each phase function, and all may be used as optimization parameters. The maximum of ninth order in x and y was made to limit the amount of computer memory required to store the coefficients of each arbitrary wavefront. In addition to using the preprogrammed phase functions described above, the designer may himself define an explicit phase function utilizing up to 100 optimization parameters. New phase functions are added to the library of available functions in this manner.

There are, of course, limitations upon how quickly any phase function which represents a recording wavefront may vary. In particular, in order that a recording wavefront not be evanescent, the following relation must be satisfied

$$\sqrt{\left(\frac{\partial\phi}{\partial x}\right)^2 + \left(\frac{\partial\phi}{\partial y}\right)^2} \leq \frac{2\pi}{\lambda} , \tag{7}$$

where λ is the recording wavelength. This is equivalent to requiring the sum of the squares of the l and m direction cosines to be no greater than unity. Similarly, in order to avoid the image ray being evanescent, from Eq. (4) it is seen that $l_I^2 + m_I^2$ must be less than unity. Violation of this constraint results in a ray failure during the ray trace.

4.1. Flat substrate

Ray tracing through a flat aspheric HOE recorded with an analytically defined arbitrary wavefront is a straightforward procedure. The direction cosines of the analytical wavefront at the reconstruction ray intercept, (x_O, y_O), are readily computed from the partial derivatives of the phase function as follows:

$$\phi = \phi(x,y)\Big|_{x_O,y_O} ; \tag{8}$$

$$l_O = \frac{\lambda}{2\pi} \frac{\partial\phi}{\partial x}\Big|_{x_O,y_O} ; \tag{9}$$

$$m_O = \frac{\lambda}{2\pi} \frac{\partial\phi}{\partial y}\Big|_{x_O,y_O} ; \tag{10}$$

and

$$n_O = \pm\sqrt{1 - l_O^2 - m_O^2} . \tag{11}$$

The sign of the z direction cosine given in Eq. (11) is chosen to provide the desired direction of propagation. Then, using the grating Eqs. (1) to (4), the phase and direction cosines of the image ray are computed.

4.2. Curved substrate

The use of an analytically defined wavefront to record an aspheric HOE on a curved substrate is somewhat more complex than the flat substrate case. One method of specifying the wavefront would be to define a phase function on the curved surface, in which case the computation of the direction cosines would depend upon the surface function in addition to the phase function (Fig. 3(a)). An alternative approach would be to define the phase function on a plane separated from the curved substrate. This latter case is similar to that of defining a wavefront by an auxiliary system in that, in order to find the ray phase and direction cosines at a given intercept, it is necessary to either perform an iterative ray trace (Fig. 3(b)) or trace a grid of rays and use interpolation. In this case, the procedure is simplified by the fact that the ray trace is between two surfaces with no intervening optics. It is particularly simple if the plane is chosen to be a tangent plane of the curved surface.

We chose to implement the first method in which the phase function is defined on the curved surface. The analysis proceeds as follows. Let the phase of a wavefront throughout a certain volume be $\hat{\phi}(x,y,z)$. Assuming that the wavefront forms a normal congruence (i.e., rays do not cross one another at the surface, and the phase and direction cosines are uniquely defined at every point), the wave vector is given by

$$\vec{k} = k_x \hat{x} + k_y \hat{y} + k_z \hat{z} = \nabla\hat{\phi}(x,y,z) , \tag{12}$$

where $\hat{x}$, $\hat{y}$, and $\hat{z}$ are the cartesian unit vectors. The direction cosines are given by

$$l = k_x/k = \frac{1}{k} \frac{\partial\hat{\phi}}{\partial x} , \tag{13}$$

$$m = k_y/k = \frac{1}{k} \frac{\partial\hat{\phi}}{\partial y} , \tag{14}$$

and

$$n = k_z/k = \frac{1}{k} \frac{\partial\hat{\phi}}{\partial z} , \tag{15}$$

where

$$k = |\vec{k}| = \frac{2\pi}{\lambda} , \tag{16}$$

where λ is the wavelength of light in the medium. The phase evaluated at a surface

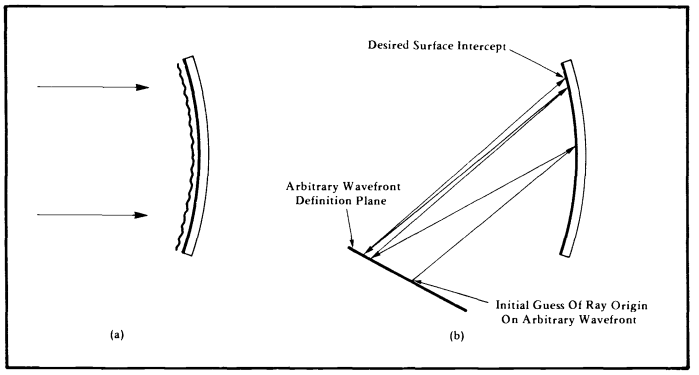

Fig. 3. A curved aspheric HOE recorded with an analytically defined wavefront can have that wavefront (a) defined on the curved surface or (b) defined on a plane separated from the surface.

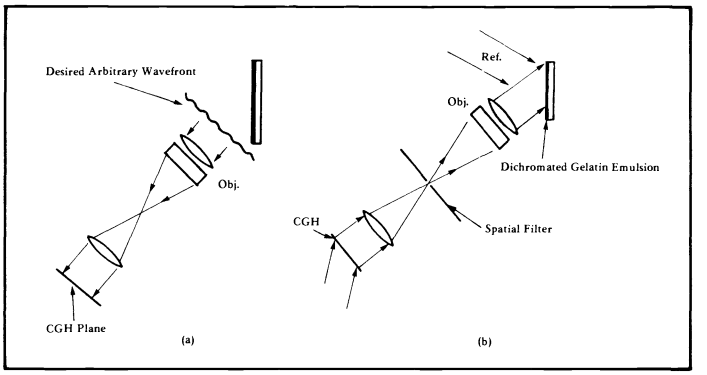

Fig. 4. COHOE recording process. (a) After the desired arbitrary recording wavefront is defined, it is backwards ray traced through an auxiliary recording system to a CGH definition plane. (b) The COHOE is recorded on a high efficiency medium using the CGH and optical system as defined in (a).

$$z = z(x,y) \tag{17}$$

is given by

$$\phi(x,y) = \hat{\phi}\left[x, y, z(x,y)\right], \tag{18}$$

which we refer to as the surface phase function. Having defined the surface phase function $\phi(x,y)$ by an analytical expression, the problem is to recover the direction cosines which are proportional to the partial derivatives of $\hat{\phi}(x,y,z)$, which are different from the partial derivatives of $\phi(x,y)$. By the chain rule of partial derivatives, we have the two equations

$$\frac{\partial \phi}{\partial x} = \phi_x = \frac{\partial \hat{\phi}}{\partial x} + \frac{\partial \hat{\phi}}{\partial z}\frac{\partial z}{\partial x} \tag{19}$$

and

$$\frac{\partial \phi}{\partial y} = \phi_y = \frac{\partial \hat{\phi}}{\partial y} + \frac{\partial \hat{\phi}}{\partial z}\frac{\partial z}{\partial y}, \tag{20}$$

and, in addition, taking the magnitude squared of Eq. (12) we have the condition

$$k^2 = \left(\frac{\partial \hat{\phi}}{\partial x}\right)^2 + \left(\frac{\partial \hat{\phi}}{\partial y}\right)^2 + \left(\frac{\partial \hat{\phi}}{\partial z}\right)^2. \tag{21}$$

Solving the three simultaneous Eqs. (19), (20), and (21) for the three unknowns, we find that

$$\frac{\partial \hat{\phi}}{\partial z} = \hat{\phi}_z =$$

$$\frac{(\phi_x z_x + \phi_y z_y) \pm \sqrt{(\phi_x z_x + \phi_y z_y)^2 + (1+z_x^2+z_y^2)\,(k^2-\phi_x^2-\phi_y^2)}}{(1+z_x^2+z_y^2)}, \tag{22}$$

$$\frac{\partial \hat{\phi}}{\partial x} = \phi_x - \hat{\phi}_z z_x, \tag{23}$$

and

$$\frac{\partial \hat{\phi}}{\partial y} = \phi_y - \hat{\phi}_z z_y, \tag{24}$$

where $z_x = \partial z(x,y)/\partial x$, and $z_y = \partial z(x,y)/\partial y$. The computation of the phase and direction cosines from the surface phase function using Eqs. 22 to 24 is very straightforward in contrast with the method of defining the phase on a plane separated from the curved surface. Unlike the latter method, however, the definition of the phase on a curved surface causes a strong coupling between the wavefront $\hat{\phi}(x,y,z)$ and the shape of the surface $z(x,y)$, for a given $\phi(x,y)$.

5. RECORDING TECHNIQUES FOR ASPHERIC HOEs

Once a recording wavefront is established by the designer, it becomes necessary to produce that wavefront in the laboratory. For the case of a recording wavefront defined by an auxiliary system as depicted in Fig. 2(a), the procedure is straightforward: an optical system corresponding to the auxiliary system must be assembled. For the case of an analytically defined arbitrary wavefront, on the other hand, the design itself does not suggest a method of arriving at the desired wavefront.

One method of arriving at a desired wavefront would be to record the aspheric HOE as a CGH.[4] Several inherent limitations of CGHs, however, severely limit the direct use of a CGH as a HOE in an optical system. First and foremost, optical recording devices used to generate CGHs are limited in spatial resolution and space-bandwidth product, thus restricting the angles of diffraction and numerical apertures of the CGH. In addition, unwanted orders of diffraction and other spurious terms are usually present in a CGH. These further restrict the usable diffraction angles and field-of-view if interference with these undesired terms is to be avoided. Another limitation is the low value of the maximum diffraction efficiency for most types of GCHs. The maximum diffraction efficiency for a thin amplitude hologram is 6.25%, for a binary amplitude hologram 10.13%, and for a thin phase hologram 33.9%.[5] Types of CGHs that have diffraction efficiencies approaching 100%, such as the kinoform[6] and the ROACH,[7] are more difficult to generate accurately.

All of the above limitations can be circumvented, however, through the use of a HOE recorded with a CGH in one of the recording beams, instead of using the CGH itself as the optical element. By using a volume phase material, such as dichromated gelatin for the HOE,[8] diffraction efficiencies approaching 100% are achieved and spurious orders of diffraction are minimized. By combining appropriate optics with the CGH in the recording beam, the resolution and the space-bandwidth product required of the CGH can be greatly reduced.[9] In addition, spatial filtering can be performed in order to remove spurious terms inherent in the CGH. Assuming that the recording wavefront of the HOE has already been specified as an analytical arbitrary wavefront, the first step is to design a recording system that reduces the space-bandwidth product and resolution requirements of the CGH. Then the ray-trace program is used to back-propagate the desired recording wavefront through a recording optical system to a CGH plane (Fig. 4(a)). The recording optical system will ordinarily be designed to remove tilt, focus, and other low-order phase terms which tend to be large in magnitude. A secondary purpose of the recording optical system is

to provide a frequency plane in which a spatial filter may be used to remove the undesired diffracted orders of the CGH. Once the recording optical system is designed to produce a wavefront with acceptably low space-bandwidth product at the CGH plane, a grid of rays is back-propagated from the hologram to the CGH plane to provide samples of the phase function that is to be recorded as a CGH. A frequency offset must be added during the CGH recording process to insure that the zero-order and second-order diffracted terms do not overlap the desired first-order diffracted term in the frequency plane. The amplitude transmittance of the CGH is made to have the form

$$t_a(x,y) = b + m(x,y) \cos\left[\omega x + \phi(x,y)\right] , \tag{25}$$

where $b \simeq 0.5$ is a bias, $m \leq 0.5$ is the modulation, and ωx is the carrier frequency offset. The amplitude of the wavefront in the CGH plane is proportional to the modulation. For this Burch-type[10] CGH (simple carrier frequency), an offset slightly larger than one half of the double-sided bandwidth of the wavefront is required. This is less than that generally required by an optically generated hologram because the Burch-type CGH does not record the object autocorrelation term (ordinarily encountered in holography) which has twice the bandwidth of the object wavefront. However, in order to avoid spurious terms that would arise in the event of a nonlinear amplitude transmittance, it may be necessary to use a carrier frequency that is 1.5 times the double-sided bandwidth of the wavefront.[5] It is assumed that the effects of film nonlinearities are minimized by precompensating for them in the recording of the CGH.

Finally, the CGH is fabricated and assembled with the recording system (Fig. 4(b)) to provide the desired recording wavefront at the HOE. We call the HOE which is recorded in this manner a computer-originated HOE (COHOE). In the following sections we discuss an example of the design of an aspheric HOE and its implementation as a COHOE.

6. AN ASPHERIC HOE DESIGN EXAMPLE

To demonstrate the use of an analytical arbitrary recording wavefront, we designed a Fourier transform HOE which could be used in a coherent optical processor (Fig. 5). A transparency at the input plane is illuminated by a coherent plane wavefront. The input transparency produces an angular spectrum of plane wavefronts (one for each spatial frequency component of the input) which propagate to the Fourier transform HOE. The HOE causes them to be focused to points in the output plane. The higher spatial frequencies in the input transparency diffract the illuminating wavefront at proportionally higher angles and come to focus farther from the center of the output plane.

In a previous design effort to produce such a Fourier transform HOE using conventional spherical wavefronts,[11] it was determined that optimum performance over a range of input spatial frequencies was achieved with a recording geometry as shown in Fig. 6. The point source for the object recording wavefront should be on an axis normal to the HOE at a point corresponding to the center of the output plane.

Using this previous design as a starting point, we further optimized the HOE, allowing the tilted plane reference wavefront to be perturbed by the following polynomial phase function:

$$\begin{aligned}\phi(x,y) = 2\pi \left[C_{20}x^2 + C_{40}x^4 + C_{60}x^6 + C_{80}x^8 \right. \\ + C_{02}y^2 + C_{04}y^4 + C_{06}y^6 + C_{08}y^8 \\ \left. + C_{22}x^2y^2 + C_{44}x^4y^4 \right] .\end{aligned} \tag{26}$$

(In Figs. 5 and 6, the x dimension of the HOE is in the plane of the page, and the y dimension is into the page.) All ten of the C_{ij} coefficients were allowed to vary during a damped least-squares optimization. Twenty-one rays forming a pair of orthogonal fans on a 25 mm diameter input aperture (Fig. 7) were ray traced to the

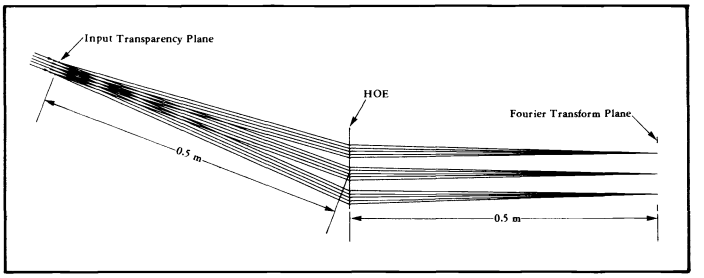

Fig. 5. Fourier transform HOE readout geometry. Three bundles of five parallel input rays each are shown propagating from the input plane to Fourier transform plane. Each of the three ray bundles represents a different plane-wave spatial frequency component which comes to focus at a point in the transform plane.

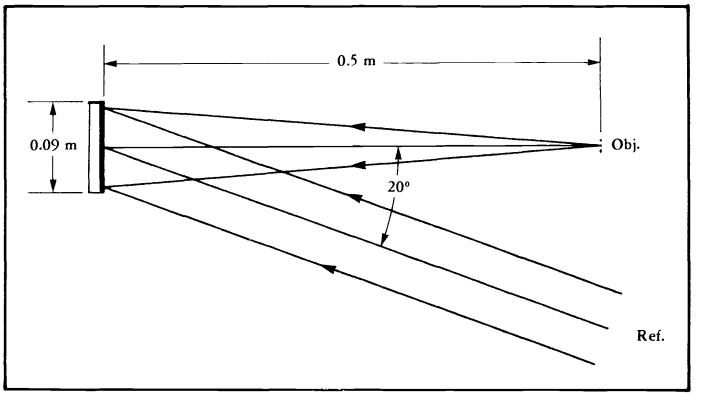

Fig. 6. The optimized recording geometry for a conventional Fourier transform HOE using plane and spherical wavefronts.

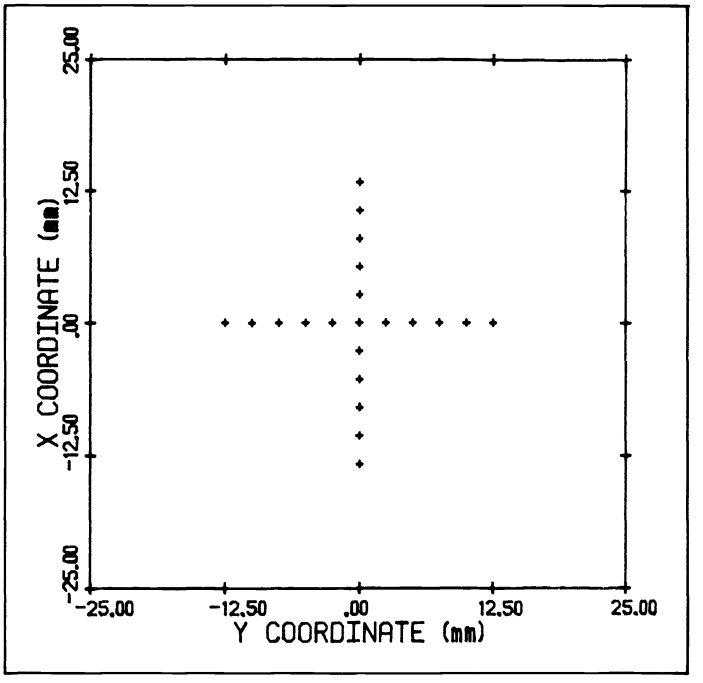

Fig. 7. Ray-trace input ray distribution used for aberration calculations (orthogonal fans).

Fourier transform plane for each of ten illumination angles during each system solution. The focal length of the HOE was designed to be 0.5 meters, and the recording and readout wavelengths were both 514.5 nm. The merit function consisted of the sum of squares of rms spot sizes at the Fourier transform plane for ten illumination angles:

TABLE I. Optimized Coefficients for an Aspheric Fourier Transform HOE

$C_{20} = .714$	$C_{02} = 1.569$	$C_{22} = 1.908$
$C_{40} = 4.092$	$C_{04} = 2.194$	$C_{44} = 64.619$
$C_{60} = 3.150$	$C_{06} = 4.036$	
$C_{80} = -.964$	$C_{08} = .502$	

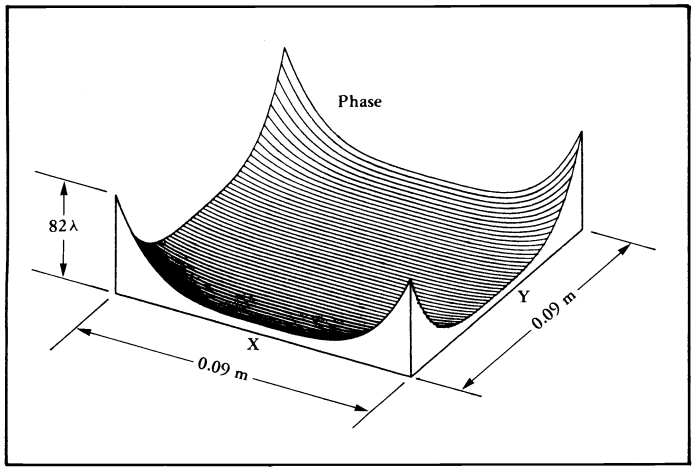

Fig. 8. Three-dimensional plot of the optimized aspheric phase correction to the reference recording wavefront of a Fourier transform HOE (as defined by Table I).

$\alpha = -2.4°, -1.2°, 0°, 1.2°, 2.4°$ (in the x-z plane), and $\beta = -2.4°, -1.2°, 0°, 1.2°, 2.4°$ (in the y-z plane). The resultant optimized coefficients are given in Table I. The coefficients of Table I are normalized to have units of wavelengths, and the x and y coordinates are scaled such that $-1 \leq x, y \leq 1$ over the hologram recording area of 90 mm by 90 mm (i.e., x and y are unitless). A perspective plot of the optimized phase correction is shown in Fig. 8. Aberration plots which compare the primary aberrations of the starting design (conventional spherical HOE) and the optimized aspheric HOE as a function of illumination angle (x-z plane) are depicted in Fig. 9.

The conventional HOE design exhibits large amounts of field curvature and coma and essentially no spherical aberration. The aspheric HOE design has significantly reduced the field curvature and coma at the expense of introducing some spherical aberration. The total rms aberration shows a reduction from a peak of 0.297 wavelengths for the conventional HOE to a peak of 0.038 wavelengths for the aspheric HOE design. Similarly, the rms spot size was reduced from a peak of 40.17 μm for the conventional HOE to a peak of 6.56 μm for the aspheric HOE design. The diffraction-limited spot size would be 10.29 μm. (Diffraction effects on the spot size were not considered in the geometrical ray trace.) No attempt was made to reduce distortion, although this would be possible with the proper merit function. The next section will describe an experimental verification of the design results presented in this section.

7. RECORDING AND EVALUATION OF AN ASPHERIC HOE

The aspheric Fourier transform HOE design described in the previous section was recorded as a COHOE using the optical system diagrammed in Fig. 10. The diffracted wavefront from the CGH is reimaged at the COHOE recording plane by a one-to-one telescope. This telescope not only performs imaging from the CGH plane to the COHOE plane, but it also preserves the desired phase relationships (i.e., it does not introduce an extra spherical phase term as would imaging with a single lens). For this case, it was assumed that the imaging system adds no extra phase terms, so in the design it was not necessary to simulate the effects of the imaging system. A spatial

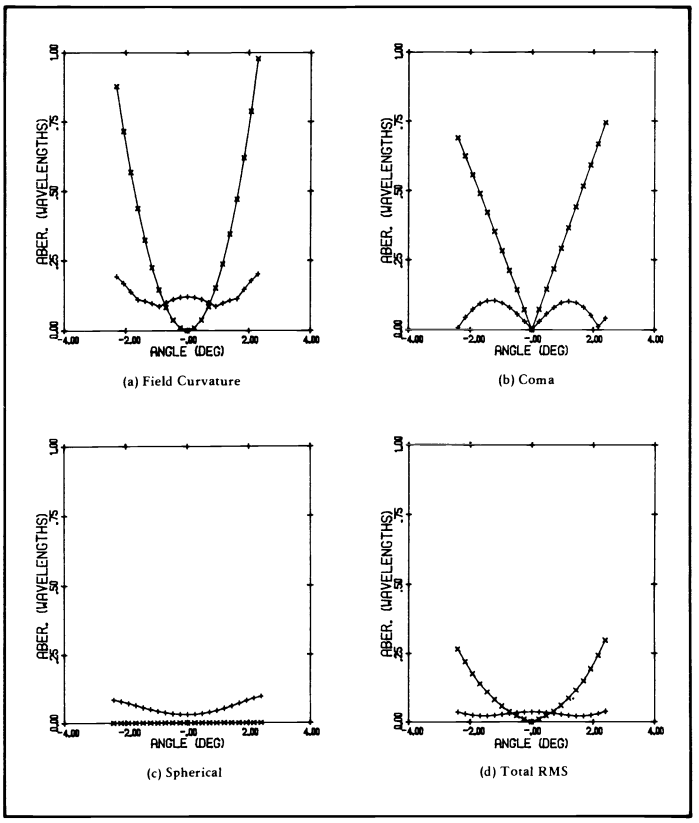

Fig. 9. Aberration plots comparing the performance of a conventional Fourier transform HOE (x's) and an aspheric Fourier transform HOE (+'s).

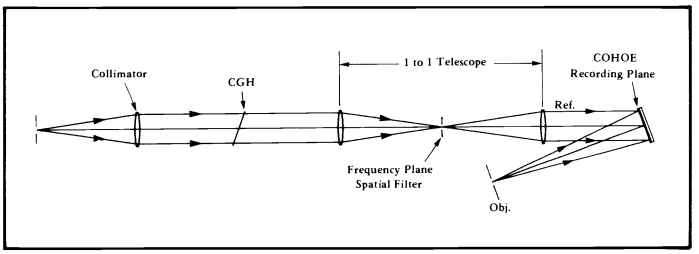

Fig. 10. The COHOE recording geometry used to produce a Fourier transform HOE with an aspheric reference wavefront as defined by Table I.

filter mask is positioned at the frequency plane such that only the desired first-order diffracted wavefront of the CGH is passed to the recording plane. The tilt of the COHOE is such that the desired 20° offset angle is obtained at the recording plane. A slight additional tilt is added to allow for the angle that the first-order diffracted term makes with the optical axis as it exits from the telescope. The CGH is similarly tilted so that it and the COHOE are in conjugate image planes. An objective and pinhole assembly provide the required point source object beam.

The optimized arbitrary recording wavefront described by Eq. (26) and Table I has maximum bandwidths of 0.747 cyc/mm in the x dimension and 0.758 cyc/mm in the y dimension when evaluated over a 90 mm diameter aperture. This wavefront was recorded as a CGH on an Optronics Model 1600 film recorder after a carrier frequency of 3 cyc/mm and a bias were added. The film recorder was operated with a 50-μm-square recording spot on a 50 μm sample spacing. The Optronics Model 1600 film recorder is also capable of recording a 25-μm-square spot on a 25 μm sample spacing with reduced speed. The Optronics film recorder has a rotating drum with a translating light-emitting diode (LED) and uses Kodak Linagraph Shellburst film #2474. The CGH was contact copied onto a Kodak

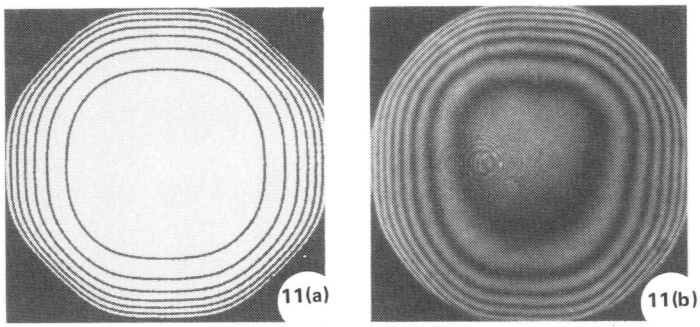

Fig. 11. Interferograms of the aspheric wavefront defined by Table I (a) as predicted by a computer ray trace and (b) as optically recorded.

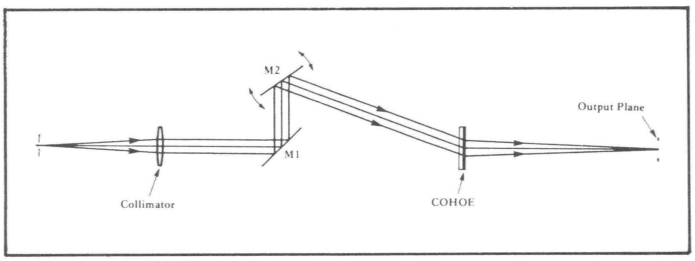

Fig. 12. Optical arrangement for evaluating the performance of the aspheric Fourier transform COHOE using a rotatable mirror (M2) at the input transparency plane to simulate any single planewave spatial frequency component.

#649F microflat plate for insertion into the COHOE recording system. The microflat substrate minimized undesired phase errors due to variations in substrate thickness. Similarly, the COHOE was recorded on a Kodak #131-01 microflat plate to insure that phase errors were not introduced during readout. The recording of the COHOE utilized 514.5 nm light from an argon-ion laser. A computer-predicted interferogram of the desired wavefront correction was plotted (Fig. 11(a)) and compared with an optically derived interferogram of the wavefront as recorded by the COHOE (Fig. 11(b)). The agreement was very good, indicating that no significant phase errors were inadvertantly introduced by the recording system.

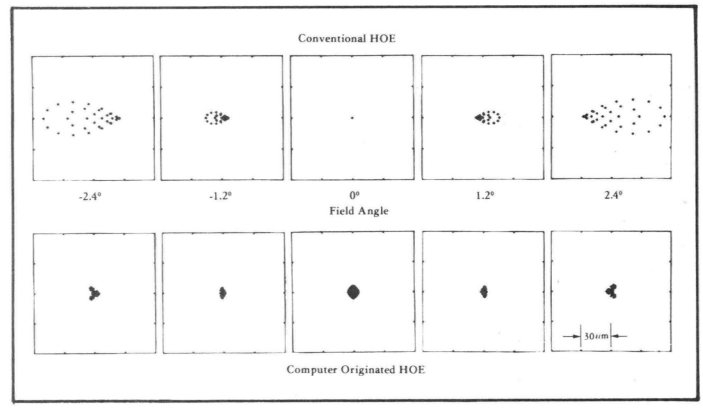

Fig. 13. Computer-predicted spot sizes of the conventional and computer-originated Fourier transform HOEs.

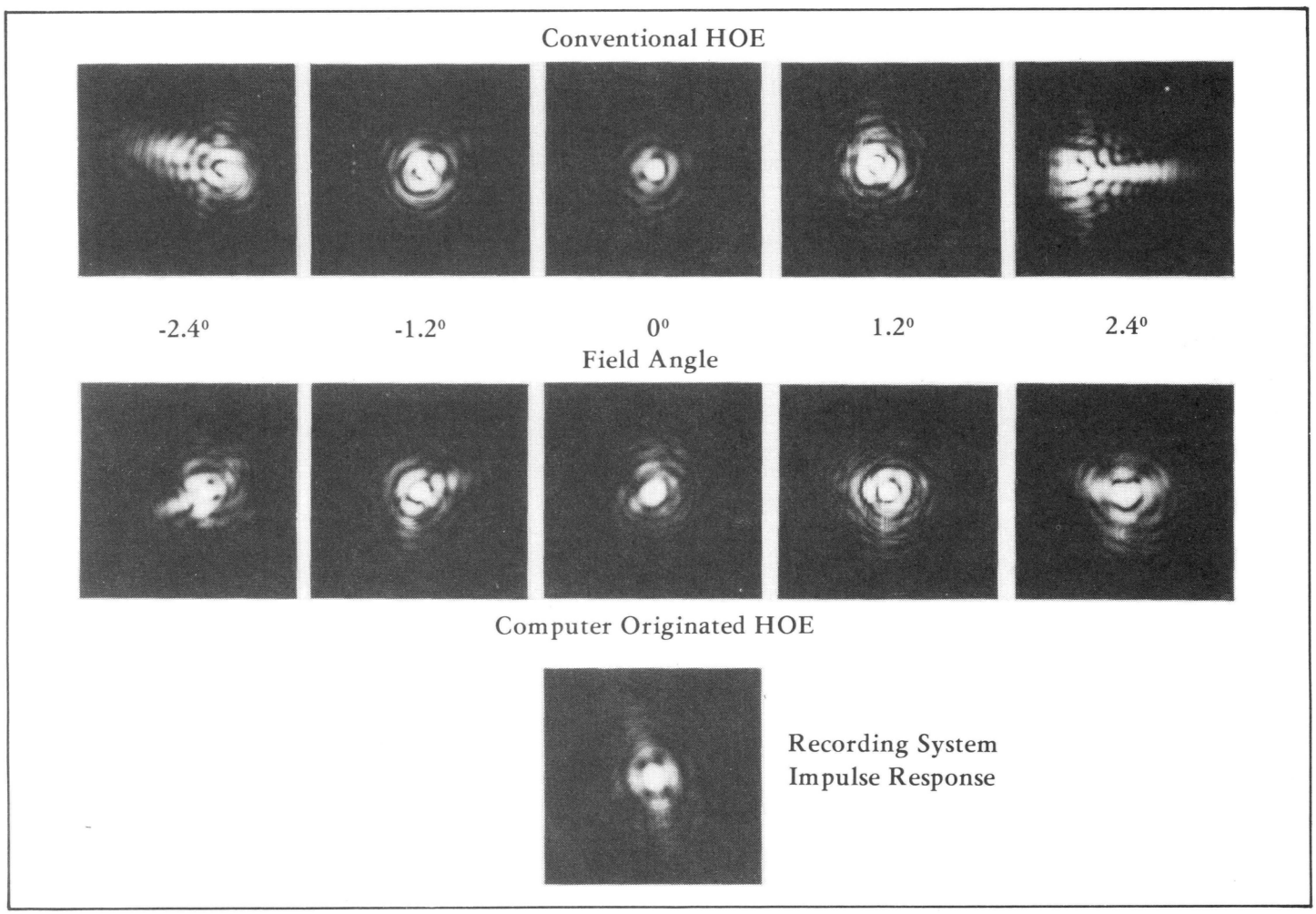

Fig. 14. Optically recorded spot sizes of the conventional and computer-originated Fourier transform HOEs using the setup shown in Fig. 12.

The performance of the COHOE was evaluated using a rotatable mirror positioned at the input transparency plane (Fig. 12). In this manner, a single stationary plane wavefront was made to simulate the wavefront that would be produced by any single spatial frequency at the input transparency plane. A microscope attached to a precision translation device was positioned such that it was focused on the Fourier transform plane of the COHOE. The rotatable mirror was positioned sequentially at the design field angles, and the resulting spot sizes in the Fourier transform plane were recorded on film. A comparison of the computer-predicted spot sizes of Fig. 13 with the corresponding measured spot sizes of Fig. 14 indicates very good agreement. The computer-generated spot diagrams were generated by ray tracing a hexapolar distribution of rays (Fig. 15) at each of the specified field angles. These spot measurements were made with an input aperture size of 35.6 mm which is somewhat larger than the design size of 25.4 mm. The impulse response of the COHOE recording system has been included in Fig. 14 for comparison. The predicted improvement in performance of the COHOE as compared with the conventional (spherical) HOE, particularly at the large field angles, is verified.

8. CONCLUSIONS

In summary, the work reported in this paper has demonstrated the feasibility of designing, analyzing, and implementing aspheric holographic optical elements using analytic descriptions of the recording wavefronts during the design phase and using a CGH in the recording beam during fabrication. The inherent properties of computer-generated holograms which limit their direct use as holographic optical elements are avoided by using the COHOE recording technique. An aspheric Fourier transform HOE was designed which demonstrated a significant improvement in performance when compared to a conventional HOE recorded with spherical wavefronts. It is our opinion that aspheric HOEs will prove to be generally valuable in the design of future high-performance holographic optical systems. In particular, we expect that aspheric HOEs will provide better performance with fewer elements and will lessen the burden on the refractive optics in hybrid systems.

9. ACKNOWLEDGMENTS

The authors wish to acknowledge useful discussions with W. Colburn and his numerous contributions to the HOAD ray-trace program. This work was supported by the U.S. Army Research Office under contract DAAG29-77-C-0017.

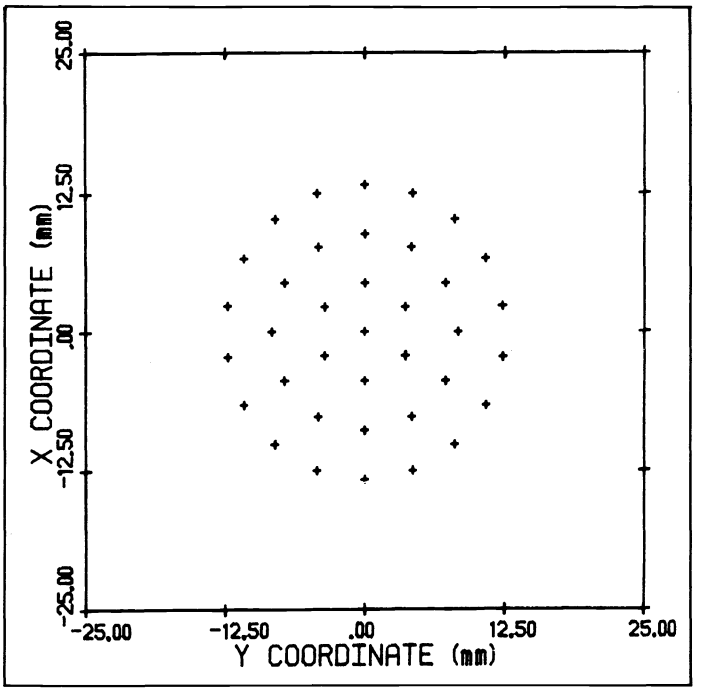

Fig. 15. Ray-trace input ray distribution used for spot diagrams (hexapolar array).

10. REFERENCES

1. W. H. Lee, "Computer-Generated Holograms: Techniques and Applications," in E. Wolf, ed., *Progress in Optics*, Vol. 16, North-Holland, Amsterdam (1978).
2. J. N. Latta and R. C. Fairchild, Proc. SPIE 39, 107 (1973); J. N. Latta, Appl. Opt. 10, 2698 (1971).
3. J. R. Fienup, Interim Scientific Report, AFOSR/NE contract FF44620-76-C-0047, ERIM Report No. 119400-1-T, March, 1977.
4. T. S. Huang, Proc. IEEE 59, 1335 (1971).
5. R. J. Collier, C. B. Burckhardt, and L. H. Lin, *Optical Holography*, Academic Press, New York (1971).
6. L. B. Lesem, P. M. Hirsch, and J. A. Jordan, Jr., IBM J. Res. Develop. 13, 150 (1969).
7. D. C. Chu, J. R. Fienup, and J. W. Goodman, Appl. Opt. 12, 1386 (1973); D. C. Chu and J. R. Fienup, Opt. Eng. 13, 189 (1974).
8. B. J. Chang and C. D. Leonard, Appl. Opt. 18, 2407 (1979).
9. S. Lowenthal and P. Chavel, Appl. Opt. 13, 718 (1974).
10. J. J. Burch, Proc. IEEE 55, 599 (1967).
11. J. R. Fienup and C. D. Leonard, Appl. Opt. 18, 631 (1979).